



A study of curvature theory for different symmetry classes of Hamiltonian

Y R KARTIK^{1,2}, RANJITH R KUMAR^{1,2}, S RAHUL^{1,2} and SUJIT SARKAR^{1,*}

¹Theoretical Sciences Division, Poornaprajna Institute of Scientific Research, Bidalur, Bengaluru 562 164, India

²Graduate Studies, Manipal Academy of Higher Education, Madhava Nagar, Manipal 576 104, India

*Corresponding author. E-mail: sujit.tifr@gmail.com

MS received 22 September 2020; revised 18 February 2021; accepted 26 February 2021

Abstract. We study and present the results of curvature for different symmetry classes (BDI, AIII and A) of model Hamiltonians and also present the transformation of model Hamiltonian from one distinct symmetry class to the other based on the curvature property. We observe the mirror symmetric curvature for the Hamiltonian with BDI symmetry class but there is no evidence of such behaviour for Hamiltonians of AIII symmetry class. We show the origin of torsion and its consequences on the parameter space of topological phase of the system. We find the evidence of torsion for the Hamiltonian of A symmetry class. We present Serret–Frenet equations for all model Hamiltonians in \mathbf{R}^3 space. To the best of our knowledge, this is the first application of curvature theory to the model Hamiltonian of different symmetry classes which belong to the topological state of matter.

Keywords. Curvature theory; torsion; topological state of matter.

PACS Nos 03.65.Vf; 02.40.–k; 73.22.Gk

1. Introduction

Symmetry and topology are two prominent branches of physics that reveal many interesting features. It is believed that these two branches are always in agreement with each other [1–7]. Before the discovery of topological phases of matter, Landau theory of symmetry breaking was considered as the prominent tool to characterise the phases of matter. But thereafter the concept got modified. There is no order parameter in topological states of systems. However, if a system is invariant under some symmetry, it gives rise to invariant quantities. These invariants can be used to characterise the topological states of matter. Based on these invariants, a system can be classified into ten distinct symmetry classes. Out of these ten non-interacting symmetry classes, only a few exhibit topological nature in 1D [4]. Recently, there were some interesting studies which involve the interplay and relations between different symmetry classes [8–11].

Differential geometry deals with the study of problems using differential calculus, integral calculus and linear algebraic techniques [12–14]. Differential geometry is a significant mathematical structure of general theory of relativity using which the concept of manifold,

curved space–time, gravity can be explained much efficiently [15–17]. There are some notable works which explained PT symmetric systems through differential geometry [18].

Curvature study is an important step in differential analysis of the system and it is effectively used in thermodynamics and many-body systems to explain its nature. Curvature is a tool to measure how curved a curve is. In other words, curvature measures the extent to which a curve deviates from a straight line. For a unit speed curve $\gamma(t)$, where t is a parameter, curvature $\kappa(t)$ at a point is defined to be $||\dot{\gamma}(t)||$ [19]. The main motivation is to explain the many-body system in a more rigorous manner. Curves and angles are effective ways of expressing the geometric properties of a physical system [20–22]. Torsion is a natural quantity which is associated with the curvature. It affects periodicity, spin wave dynamics and structural defects of the system [23–25]. Torsion also has a significant role in the dynamics of the adiabatic system, transport properties and bulk–boundary correspondence in the topological state of matter [26,27].

The geometrical studies of condensed matter systems have been an interesting area of research which has rapidly picked up pace when the principles of topology

and geometry were involved in the foundations of quantum condensed matter systems [28,29]. The physics of geometry of curves in R^3 with spins in connection with the dynamics of classical Heisenberg ferromagnetic system under different contexts has already been explored in the literature (see for example, [30–32])

The main motivation of this work is to study a few model Hamiltonians which belong to different symmetry classes from the perspective of curved space theory of differential geometry [13,14]. This paper is organised in the following manner. In §2 we introduce the model Hamiltonian and present a detailed analysis of symmetry class Hamiltonians. In §3 we present the characteristics and behaviour of parameter space curves with a detailed analysis of differential geometric study of curvature. Here we try to analyse the origin of torsion and its consequences for the present model Hamiltonian.

2. Basic model Hamiltonian

Here we consider eight model Hamiltonians belonging to different symmetry classes [8,9]. Our model Hamiltonian is expressed as

$$H = H_0 + H_{\text{eff}}, \quad (1)$$

where H_0 is the initial Hamiltonian and H_{eff} is the effective part of the Hamiltonian which is responsible for the transformation from one symmetry class to the other. Here, initial Hamiltonian H_0 is a 1D non-interacting topological insulator. We can write our Hamiltonian in the Bogoliubov–de Gennes (BdG) format as

$$H_{\text{BdG}}(k) = \chi^{(1)} \begin{pmatrix} 0 & 1 \\ 1 & 0 \end{pmatrix} + \chi^{(2)} \begin{pmatrix} 0 & i \\ -i & 0 \end{pmatrix} + \chi^{(3)} \begin{pmatrix} 1 & 0 \\ 0 & -1 \end{pmatrix}. \quad (2)$$

The components can be written as $\chi^{(1)} = 0$, $\chi^{(2)} = \Delta \sin k$ and $\chi^{(3)} = \mu + 2t \cos k$. The effective term (H_{eff}) is momentum-dependent, and is in the following form:

$$H_{\text{eff}} = \delta_1 k \sigma_x + \delta_2 k \sigma_y + \delta_3 k \sigma_z = \delta_i (\mathbf{k}_i \cdot \boldsymbol{\tau}_i),$$

where $k_1 = k_2 = k_3 = k$ (a detailed study is presented in ref. [8]). We consider a very specific type of effective term which is of much theoretical interest. The results of this study may motivate researchers in quantum simulation studies to look for this type of effective term and consequences of their effects on the topological state of matter [33–35].

2.1 Hamiltonian $H^{(1)}(k)$ when $\delta_1 = \delta_2 = \delta_3 = 0$

Here the effective part of the Hamiltonian is zero. So, the Hamiltonian in Pauli basis can be written as

$$H_k^{(1)} = 2\Delta \sin k \sigma_y + (2t \cos k + \mu) \sigma_z. \quad (3)$$

Hamiltonian in matrix form can be written as

$$\mathcal{H}^{(1)}(k) = \begin{pmatrix} 2t \cos(k) + \mu & 2i \Delta \sin(k) \\ -2i \Delta \sin(k) & -2t \cos(k) - \mu \end{pmatrix}. \quad (4)$$

2.2 Hamiltonian $H^{(2)}(k)$ when $\delta_1 = \delta_3 = 0$, $\delta_2 \neq 0$

Here the effective term is added to the σ_y component of the Hamiltonian. It can be written in terms of Pauli basis as

$$H_k^{(2)} = (2\Delta \sin k + \delta_2 k) \sigma_y + (2t \cos k + \mu) \sigma_z. \quad (5)$$

Hamiltonian in matrix form can be written as

$$\mathcal{H}^{(2)}(k) = \begin{pmatrix} 2t \cos(k) + \mu & 2i \Delta \sin(k) + i \delta_2 k \\ -2i \Delta \sin(k) - i \delta_2 k & -2t \cos(k) - \mu \end{pmatrix}. \quad (6)$$

2.3 Hamiltonian $H^{(3)}(k)$ when $\delta_3 \neq 0$, $\delta_1 = \delta_2 = 0$

Here the effective term is added to the σ_x component of the Hamiltonian. It can be written in terms of Pauli basis as

$$H_k^{(3)} = 2\Delta \sin k \sigma_y + (2t \cos k + \mu + \delta_3 k) \sigma_z. \quad (7)$$

Hamiltonian in matrix form can be presented as

$$\mathcal{H}^{(3)}(k) = \begin{pmatrix} 2t \cos(k) + \mu + \delta_3 k & 2i \Delta \sin(k) \\ -2i \Delta \sin(k) & -2t \cos(k) - \mu - \delta_3 k \end{pmatrix}. \quad (8)$$

2.4 Hamiltonian $H^{(4)}(k)$ when $\delta_1 = 0$, $\delta_2 \neq 0$, $\delta_3 \neq 0$

Here effective terms are added to both the σ_x and σ_y components of the Hamiltonian. It can be written in terms of Pauli basis as

$$H_k^{(4)} = (2\Delta \sin k + \delta_2 k) \sigma_y + (-2t \cos k - \mu + \delta_3 k) \sigma_z. \quad (9)$$

Hamiltonian $H^{(4)}(k)$ in matrix form can be presented as

$$\mathcal{H}^{(4)}(k) = \begin{pmatrix} 2t \cos(k) + \mu + \delta_3 k & 2i \Delta \sin(k) + i \delta_2 k \\ -2i \Delta \sin(k) - i \delta_2 k & -2t \cos(k) - \mu - \delta_3 k \end{pmatrix}. \quad (10)$$

2.5 Hamiltonian $H^{(5)}(k)$ when $\delta_1 \neq 0, \delta_2 = \delta_3 = 0$

Here effective term is added to the σ_x component of the Hamiltonian. It can be written in terms of Pauli basis as

$$H_k^{(5)} = (\delta_1 k)\sigma_x + (2\Delta \sin k)\sigma_y + (2t \cos k + \mu)\sigma_z. \tag{11}$$

Hamiltonian $H^{(5)}(k)$ can be written in matrix form as

$$\mathcal{H}^{(5)}(k) = \begin{pmatrix} 2t \cos(k) + \mu + \delta_3 k & 2i \Delta \sin(k) + i \delta_2 k + \delta_1 k \\ -2i \Delta \sin(k) & -2t \cos(k) - \mu - \delta_3 k - i \delta_2 k + \delta_1 k \end{pmatrix}. \tag{18}$$

$$\mathcal{H}^{(5)}(k) = \begin{pmatrix} 2t \cos(k) + \mu & 2i \Delta \sin(k) + \delta_1 k \\ -2i \Delta \sin(k) + \delta_1 k & -2t \cos(k) - \mu \end{pmatrix}. \tag{12}$$

2.6 Hamiltonian $H^{(6)}(k)$ when $\delta_1 \neq 0, \delta_2 \neq 0, \delta_3 = 0$

Here effective terms are added to both the σ_x and σ_y components of the Hamiltonian. It can be written in terms of Pauli basis as

$$H_k^{(6)} = (\delta_1 k)\sigma_x + (2\Delta \sin k + \delta_2 k)\sigma_y + (2t \cos k + \mu)\sigma_z. \tag{13}$$

Hamiltonian $H^{(6)}(k)$ can be written in matrix form as

$$\mathcal{H}^{(6)}(k) = \begin{pmatrix} 2t \cos(k) + \mu & 2i \Delta \sin(k) + i \delta_2 k + \delta_1 k \\ -2i \Delta \sin(k) - i \delta_2 k + \delta_1 k & -2t \cos(k) - \mu \end{pmatrix}. \tag{14}$$

2.7 Hamiltonian $H^{(7)}(k)$ when $\delta_1 \neq 0, \delta_2 = 0, \delta_3 \neq 0$

Here effective terms are added to both the σ_x and σ_z components of the Hamiltonian. It can be written in terms of Pauli basis as

$$H_k^{(7)} = (\delta_1 k)\sigma_x + (2\Delta \sin k + \delta_3 k)\sigma_y + (2t \cos k + \mu)\sigma_z. \tag{15}$$

Hamiltonian $H^{(7)}(k)$ can be written in matrix form as

$$\mathcal{H}^{(7)}(k) = \begin{pmatrix} 2t \cos(k) + \mu + \delta_3 k & 2i \Delta \sin(k) + \delta_1 k \\ -2i \Delta \sin(k) + \delta_1 k & -2t \cos(k) - \mu - \delta_3 k \end{pmatrix}. \tag{16}$$

2.8 Hamiltonian $H^{(8)}(k)$ when $\delta_1 \neq 0, \delta_2 \neq 0, \delta_3 \neq 0$

Here effective terms are added to the σ_x, σ_y and σ_z components of the Hamiltonian. It can be written in terms of Pauli basis as

$$H_k^{(8)} = (\delta_1 k)\sigma_x + (2\Delta \sin k + \delta_2 k)\sigma_y + (2t \cos k + \mu + \delta_3 k)\sigma_z. \tag{17}$$

Hamiltonian $H^{(8)}(k)$ can be written in matrix form as

The addition of the effective term does not affect the Hermitian property of the system.

Basically, the Hamiltonian is in the spinless fermion basis. The effective term is also in spinless basis and is momentum-dependent. Therefore, we justify the physical relevance of the effective term.

The first Hamiltonian $H_1(k)$ is the Kitaev model Hamiltonian [36] which governs the topological state of quantum matter. The other seven Hamiltonians (i.e. from $H_2(k)$ to $H_8(k)$) are variants of Kitaev model Hamiltonian. We consider these additional Hamiltonians in the spirit of theoretical studies only. Using these model Hamiltonians, we study the topological as well as geometric properties of quantum condensed matter system up to some extent.

3. Curvature analysis of curves in planar parameter space

Curvature can be defined as the rate of variation of the angle that the tangent line makes at a particular point. To call a curve as a regular curve, it should have a non-vanishing tangent line. Curve theory basically deals with analysing the basic properties of the curves. Basic properties include, the arc length, winding number with curvature and torsion of the curves [19]. Topological invariant quantities, such as winding number and Chern number depend on the topology of the parameter space, where for a particular topological configuration space, winding number acquires a definite value, and change in the winding number leads to different topological configurations of the system [37].

The understanding of the curve concept is simplified by using the differential geometry tool called curvature κ .

The relation which relates the parametrised curve $c(k)$ and the curvature $\kappa(t)$ is given by [38]

$$\kappa(k) = \frac{\det(c(\dot{k}), c(\ddot{k}))}{\|c(\dot{k})\|^3}, \tag{19}$$

where dot represents d/dk . For a unit speed curve $c : I \rightarrow \mathbb{R}^2$ where $I = [a, b]$ is a closed curve interval. Then $\dot{c}(k)$ gives the velocity vector defined by $(\cos \theta(k), \sin \theta(k))^T$ of an integer multiple of 2π , as the curve is defined in a closed interval. As the angle changes along the curve, the invariant quantity winding number is defined by $\theta(b) - \theta(a)$. If $\theta_1, \theta_2 : I \rightarrow \mathbb{R}$ satisfies the velocity equation, $\theta_1 = \theta_2 + 2n\pi$, where $n \in \mathbb{Z}$.

The velocity term $\dot{c}([a, b]) \subset \mathbb{S}_R$, i.e., $\dot{c}(t) > 0$ for all $k \in I$ and $\dot{c}(t) = (\dot{c}_1, \dot{c}_2)^T$,

$$\frac{\dot{c}_2}{\dot{c}_1} = \frac{\sin \theta(k)}{\cos \theta(k)} = \tan \theta(k)$$

and

$$\theta(k) = \arctan \left(\frac{\dot{c}_2(k)}{\dot{c}_1(k)} \right) + 2n\pi, \quad n \in \mathbb{Z}.$$

So considering $c: \mathbb{R} \rightarrow \mathbb{R}^2$ a unit speed vector of a curve with period L and $\theta: \mathbb{R} \leftarrow \mathbb{R}$ a scalar, the winding number is given by

$$w_k = \frac{1}{2\pi}(\theta(L) - \theta(0)), \tag{20}$$

where $(\theta(L) - \theta(0))$ is well defined irrespective of the choice of θ . Therefore, it is clear from the above equation that to get a complete physical picture of the winding number, the study of the curve is useful. It is well known that the topological system is a closed curve which encircles the origin. Geometrically, the parameter space of a topological system is an ellipse and defined as the locus of points such that the sum of distances from the foci is constant. The standard equation of ellipse is given by

$$\frac{x^2}{a^2} + \frac{y^2}{b^2} = 1,$$

where a and b are semi-major and semi-minor axes respectively. The parametric equation is given by $[a(k), b(k)] = (a \cos k, b \sin k)$ where $0 \leq k < 2\pi$.

The curvature of ellipse is given by [13]

$$\kappa(k) = \frac{ab}{(b^2 \cos^2 k + a^2 \sin^2 k)^{3/2}}, \tag{21}$$

where a and b are semi-major axis and semi-minor axis of ellipse respectively (figure 1). From these two parameters, we can analyse the curvature in three different cases.

First case: When $a < b$, the curvature is maximum on the semi-major axis ($-\pi/2$ and $\pi/2$) and minimum on the semi-minor axis.

Second case: When $a = b$, the parameter space curve is a circle with the constant curvature.

Third case: When $a > b$, the curvature is minimum on the semi-major axis ($-\pi/2$ and $\pi/2$) and maximum on the semi-minor axis [14].

For a plane unit speed curve $c: I \rightarrow \mathbb{R}^2$, where $n(k)$ and $\kappa(k)$ give the normal unit vector and curvature of the curve. Then,

$$(v(\dot{k}), n(\dot{k})) = (v(k), n(k)) \begin{pmatrix} 0 & -\kappa(k) \\ \kappa(k) & 0 \end{pmatrix} \tag{22}$$

defines the relation $v = k \cdot n$ and $\dot{n} = -\kappa \cdot v$, where $v = c(\dot{k})$ [13]. This is called Frenet equation which gives the information about the curvature properties of the curve $c(k)$.

For a non-vanishing curve $c(k)$ with a non-vanishing curvature $\kappa(k)$, torsion is given by [19]

$$\tau = \frac{(\dot{c}(k) \times \ddot{c}(k)) \cdot \ddot{c}(k)}{\|\dot{c}(k) \times \ddot{c}(k)\|^2}. \tag{23}$$

Our model Hamiltonian is written in the Pauli spin basis. Naturally, the quantity torsion gives the curl of the derivatives of the curve. This results in the curve opening and helical motion on the addition of the effective term αk .

To understand the kinematic properties of curve $c: \mathbb{R} \rightarrow \mathbb{R}^3$, we study Serret–Frenet equation for the curve [19]. For a unit-speed curve $c(k)$ in \mathbb{R}^3 curvature explains the failure of a curve to be a straight line and torsion explains the failure of a line to be a planar. Serret–Frenet formula describes the derivative of tangent (T), normal (N) and binormal (B) unit vectors with respect to the arc length of the parameter of the curve (s) [19], i.e.,

$$\begin{aligned} \frac{d\mathbf{T}}{ds} &= \kappa \mathbf{N} \\ \frac{d\mathbf{N}}{ds} &= -\kappa \mathbf{T} + \tau \mathbf{B} \\ \frac{d\mathbf{B}}{ds} &= -\tau \mathbf{N}. \end{aligned} \tag{24}$$

Here $\dot{\mathbf{B}}$ is perpendicular to \mathbf{T} . Being perpendicular to both \mathbf{T} and \mathbf{B} , $\dot{\mathbf{B}}$ must be parallel to \mathbf{N} . It is to be noted that, torsion (τ) exists only for a curve with non-zero curvature. Equation (24) is known as Serret–Frenet

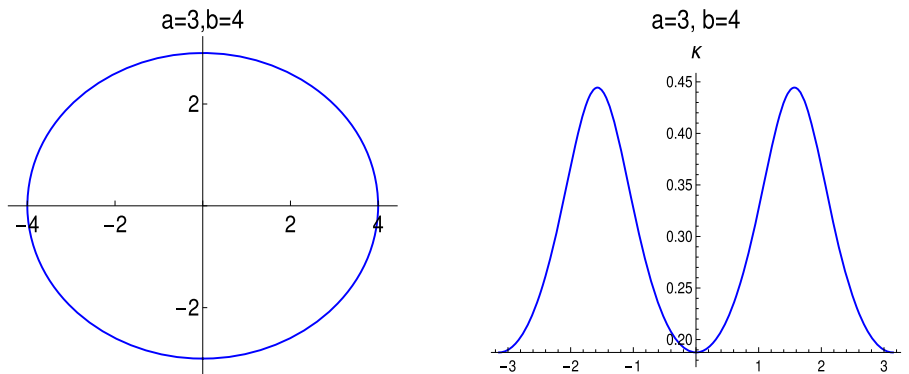


Figure 1. The graphical representation of an ellipse (left) and the corresponding curvature plots for the parameter space (right). Here we observe that the curvature is minimum at the origin but not vanishing.

Table 1. Properties of symmetry operators which are related to the present study.

Symmetry	Relation	Operator	Nature
Time reversal (T)	$[T, H] = 0$ $THT^{-1} = H$	$T = \mathcal{K}$ $T^2 = 1$	Reverses the arrow of time $T: t \rightarrow -t$
Particle–hole (C)	$\{C, H\} = 0$ $\mathcal{C}HC^{-1} = -H$	$C = \sigma_x \mathcal{K}$ $C^2 = 1$	Transformation between electron and holes (within certain energy range)
Chiral (S)	$\{S, H\} = H$ $SHS^{-1} = -H$	$S = \sigma_x$ $S^2 = 1$	Symmetric spectrum of the Hamiltonian

equation and gives a better understanding of the geometric properties of the system. One can also write the matrix representation of the Serret–Frenet equation as follows [19]:

$$\frac{d}{ds}(X) = \begin{pmatrix} 0 & \kappa(k) & 0 \\ -\kappa(k) & 0 & \tau(k) \\ 0 & -\tau(k) & 0 \end{pmatrix} (X), \tag{25}$$

where $X = (T, N, B)^T$. By expressing dT/ds , dN/ds and dB/ds in terms of T , N and B one can get skew-symmetric matrix and it follows that the vectors T , N and B are orthonormal for all values of the arc length parameter (s).

4. Different symmetry classes and their nature

Different symmetry classes have already been studied and discussed extensively [8–10]. Here, in table 1 we discuss them very briefly which are directly involved with the present study.

Time-reversal symmetry (TR): Time-reversal symmetry is the transformation which is anti-unitary in nature. The time-reversal operator just reverses the sign of momentum but does not affect the position. It is equivalent to

the complex conjugate operator (\mathcal{K}).

$$TxT^{-1} = x, \quad TkT^{-1} = -k, \quad TiT^{-1} = -i. \tag{26}$$

Time-reversal operator is the product of unitary (U) and complex conjugate operators, i.e. $T = UK$. The square of the time-reversal operator is equal to the negative of identity which yields Kramer’s degeneracy. According to that, one state is the time-reversal of another and every state is doubly degenerate. Thus, the system becomes time-reversal invariant [5,39,40].

Particle–hole (PH) symmetry: The particle–hole operator is an anti-unitary operator and in the presence of this symmetry, each eigenfunction Ψ with $E > 0$ has its particle–hole reversed partner, $C\Psi$ with $E < 0$. The PH symmetry is the intrinsic property of mean-field theory of superconductivity.

Chiral symmetry: Chiral symmetry (S) or sublattice symmetry is the product of time-reversal operator (T) and particle–hole operator (C). Based on the behaviour of Hamiltonian with the TR, PH and chiral symmetries, it is classified into 10 symmetry classes.

In table 2, we present different symmetry classes to characterise the topological states of the system for different dimensions (d). The first column presents different symmetry classes, the second, third and fourth

Table 2. Ten-fold symmetry class for a topological system. Here Θ is the time-reversal symmetry, Ξ is the particle–hole symmetry, Π is the charge conjugation symmetry and d is the dimensionality of the system.

Symmetry	d										
	Θ	Ξ	Π	1	2	3	4	5	6	7	8
A	0	0	0	0	\mathbb{Z}	0	\mathbb{Z}	0	\mathbb{Z}	0	\mathbb{Z}
AIII	0	0	1	\mathbb{Z}	0	\mathbb{Z}	0	\mathbb{Z}	0	\mathbb{Z}	0
AI	1	0	0	0	0	0	\mathbb{Z}	0	\mathbb{Z}_2	\mathbb{Z}_2	\mathbb{Z}
BDI	1	1	1	\mathbb{Z}	0	0	0	\mathbb{Z}	0	\mathbb{Z}_2	\mathbb{Z}_2
D	0	1	0	\mathbb{Z}_2	\mathbb{Z}	0	0	0	\mathbb{Z}	0	\mathbb{Z}_2
DIII	–1	1	1	\mathbb{Z}_2	\mathbb{Z}_2	\mathbb{Z}	0	0	0	\mathbb{Z}	0
AII	–1	0	0	0	\mathbb{Z}_2	\mathbb{Z}_2	\mathbb{Z}	0	0	0	\mathbb{Z}
CII	–1	–1	1	\mathbb{Z}	0	\mathbb{Z}_2	\mathbb{Z}_2	\mathbb{Z}	0	0	0
C	0	–1	0	0	\mathbb{Z}	0	\mathbb{Z}_2	\mathbb{Z}_2	\mathbb{Z}	0	0
CI	1	–1	1	0	0	\mathbb{Z}	0	\mathbb{Z}_2	\mathbb{Z}_2	\mathbb{Z}	0

columns present respectively the time-reversal, particle–hole and charge conjugation symmetries. The rest of the table is for the dimensionality (d) and the topological index system (\mathbb{Z} and \mathbb{Z}_2). Here we mention very briefly the topological characterisation of the system, and a detailed discussion can be found in refs [8–10].

Topological states of matter are characterised by the presence of time-reversal, chiral and charge conjugation symmetries. They are classified into different symmetry classes based on these symmetry operators. The edge state in the topological systems are protected by the time-reversal symmetry ($\mathcal{T}: t \rightarrow -t$) and time-reversal symmetry (commutes with the Hamiltonian, i.e., $[\mathbf{H}, \mathcal{T}] = 0$), chiral symmetry (i.e., chiral operator anticommutes with Hamiltonian, $\{\mathcal{S}, \mathbf{H}\} = 0$) and particle–hole operator (anticommutes with the Hamiltonian $\{\mathcal{S}, \mathbf{H}\} = 0$) decide whether the system is topological or not. Table 2 presents the condition and classification of different symmetry classes. We observe that our model Hamiltonians belong to three different (BDI, AIII and A) symmetry classes. We present our results of different symmetry classes in the next section.

4.1 Results of BDI symmetry class

BDI symmetry class is characterised by the commutation of time-reversal (\mathcal{T}) operator with the Hamiltonian anticommutation of other two operators like particle–hole (\mathcal{C}) and chiral (\mathcal{S}) with the Hamiltonian (eq. (2)). Here the Hamiltonians $H^{(1)}(k)$ and $H^{(2)}(k)$ belong to the BDI class [8]. The Hamiltonian $H^{(1)}(k)$ is topological in nature. The Hamiltonian $H^{(2)}(k)$ shows topologically trivial behaviour. Now we study the curvature properties of these Hamiltonians.

4.1.1 $H^{(1)}(k)$ Hamiltonian. Here we present the results of differential geometric study based on curve

theory for the BDI Hamiltonians. The matrix form of the model Hamiltonian is

$$\mathcal{H}^{(1)}(k) = \begin{pmatrix} 2t \cos(k) + \mu & 2i \Delta \sin(k) \\ -2i \Delta \sin(k) & -2t \cos(k) - \mu \end{pmatrix}. \quad (27)$$

Here the set of possible parametric equations are

$$\begin{aligned} \chi^{(1)}(H^{(1)}(k)) &= 0 \\ \chi^{(2)}(H^{(1)}(k)) &= 2\Delta \sin k, \\ \chi^{(3)}(H^{(1)}(k)) &= 2t \cos k + \mu, \end{aligned} \quad (28)$$

H_{BdG} Hamiltonian in the pseudospin basis is

$$H^{(1)}(k) = \chi^{(2)}(H^{(1)}(k))\sigma_y + \chi^{(3)}(H^{(1)}(k))\sigma_z. \quad (29)$$

In terms of vectors, one can write the above equation as $H_{\text{BdG}} = \vec{\chi}(k) \cdot \vec{\tau}$, where $\vec{\tau}$ are the Pauli spin matrices acting in the particle–hole (Nambu) basis of H_{BdG} [41]. The energy dispersion relation

$$E^{(1)}(k) = \sqrt{(2t \cos k + \mu)^2 + (2\Delta \sin k)^2}.$$

Considering the parametric equation of the Hamiltonian $H^{(1)}(k)$ in the matrix form

$$\begin{aligned} c(k) &= \begin{bmatrix} 2\Delta \sin k \\ 2t \cos k + \mu \end{bmatrix}, \quad \dot{c}(k) = \begin{bmatrix} 2\Delta \cos k \\ -2t \sin k \end{bmatrix}, \\ \ddot{c}(k) &= \begin{bmatrix} -2\Delta \sin k \\ -2t \cos k \end{bmatrix}. \end{aligned} \quad (30)$$

Curvature is given by

$$\begin{aligned} \kappa &= \frac{\det[\dot{c}, \ddot{c}]}{\|\dot{c}\|^3} = \frac{\det \begin{pmatrix} 2\Delta \cos k & -2\Delta \sin k \\ -2t \sin k & -2t \cos k \end{pmatrix}}{\left(\sqrt{4t^2 \sin^2 k + 4\Delta^2 \cos^2 k}\right)^3} \\ &= \frac{-2t\Delta}{\left(\sqrt{t^2 \sin^2 k + \Delta^2 \cos^2 k}\right)^3}. \end{aligned} \quad (31)$$

Figure 2 represents the curvature plot for Hamiltonian $H^{(1)}(k)$. The parameter space curve for the Hamiltonian

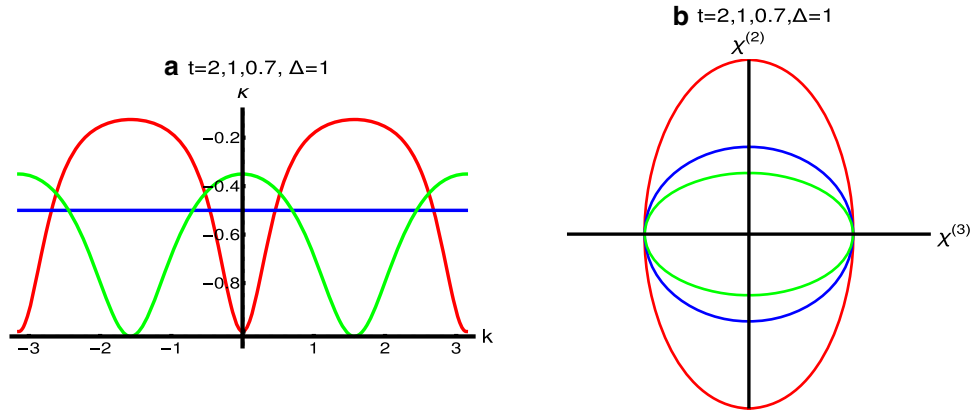


Figure 2. The left figure represents the plots of curvature with k for $\gamma = 2, 1, 0.7$ for red, blue and green respectively. The right figure represents the corresponding parameter plots for $\mu = 0$.

$H^{(1)}(k)$ is nothing but an ellipse (figure 1) due to the mathematical structure of the parametric equation.

When $\mu = 0$, the system remains in the topological state. We can study the curvature of parameter space curve for all the Hamiltonians. We cannot characterise the topological and non-topological states of the Hamiltonian from the curvature study because the curvature expression does not include the term μ . From the above general discussion on the ellipse we can characterise the parameter space curve of the $H^{(1)}(k)$ Hamiltonian into similar three cases which is described below. This is completely a theoretical study to understand the behaviour of the parameter space curve of the model Hamiltonians from the perspective of differential geometry.

First case: When $t < \Delta$, the curvature is maximum on the semi-major axis ($-\pi/2$ and $\pi/2$) and minimum on the semi-minor axis.

Second case: When $t = \Delta$, the parameter space curve is a circle with constant curvature.

Third case: When $t > \Delta$, the curvature is minimum on the semi-major axis ($-\pi/2$ and $\pi/2$) and maximum on the semi-minor axis.

4.1.2 $H^{(2)}(k)$ Hamiltonian. Hamiltonian $H^{(2)}(k)$ can be written in the matrix form as

$$\mathcal{H}^{(2)}(k) = \begin{pmatrix} 2t \cos(k) + \mu & 2i \Delta \sin(k) + i \delta_2 k \\ -2i \Delta \sin(k) - i \delta_2 k & -2t \cos(k) - \mu \end{pmatrix}. \quad (32)$$

Here the set of parametric equations are

$$\begin{aligned} \chi^{(1)}(H^{(2)}(k)) &= 0 \\ \chi^{(2)}(H^{(2)}(k)) &= 2\Delta \sin k + \delta_2 k, \\ \chi^{(3)}(H^{(2)}(k)) &= 2t \cos k + \mu. \end{aligned} \quad (33)$$

H_{BdG} Hamiltonian in the pseudospin basis is [41]

$$H^{(2)}(k) = \chi^{(2)}(H^{(2)}(k))\sigma_y + \chi^{(3)}(H^{(2)}(k))\sigma_z. \quad (34)$$

The energy dispersion relation

$$E^{(2)}(k) = \sqrt{(2t \cos k + \mu)^2 + (2\Delta \sin k + \delta_2 k)^2}.$$

Hence, the curvature for $H^{(2)}(k)$ is

$$\begin{aligned} \kappa &= \frac{\det \begin{bmatrix} 2\Delta \cos k + \delta_2 & -2\Delta \sin k \\ -2t \sin k & -2t \cos k \end{bmatrix}}{\left(\sqrt{(2t \sin k)^2 + (2\Delta \cos k + \delta_2)^2}\right)^3} \\ &= \frac{-4t \Delta - 2\delta_2 t \cos k}{\left(\sqrt{(2t \sin k)^2 + (2\Delta \cos k + \delta_2)^2}\right)^3}. \end{aligned} \quad (35)$$

Equation (35) is the analytical expression of the curvature for the Hamiltonian $H^{(2)}(k)$.

Figure 3 consists of two panels for two different values of δ_2 . The upper and lower panels represent the parameter space $\delta_2 = 0.5$ and $\delta_2 = 1$ respectively. Each panel consists of two figures, the left one is for curvature and the right one is for the corresponding parameter space curves. We observe that as value of δ_2 increases, the curvature also increases. Here we observe an interesting feature that the curvature as well as parameter plots are mirror symmetric about κ -axis. This is true for both Hamiltonians of BDI symmetry class. The parameter space curve splits into two as we increase the value of δ_2 .

The parameter space curves of Hamiltonian $H^{(2)}(k)$ resembles the cycloidal pattern due to its mathematical structure. The general expression of the cycloid is given by [14]

$$\text{Cyc}[a, b](t) = (at - b \sin t, a - b \cos t). \quad (36)$$

In general, the cycloid is classified into two categories depending on the values of coefficients. In eq. (36), if $a < b$, then the cycloid is prolate and if $a > b$, it

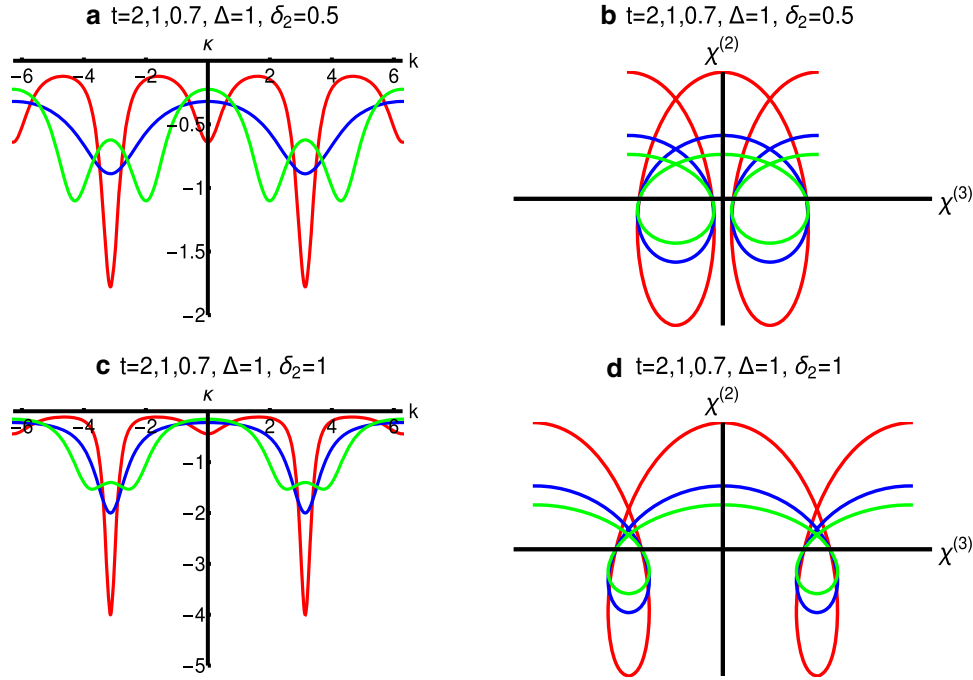


Figure 3. (a) Plots of curvature (κ) with k for $\delta_2 = 0.5$, (b) the corresponding parameter plots for the curvature plot (a), (c) plots of curvature (κ) with k for $\delta_2 = 1$ and (d) the corresponding parameter plots for the curvature plot (c). In all the plots, the red, blue and green curves represent $t = 2, 1, 0.7$ respectively.

is curate. From this classification, we can assign our Hamiltonian $H^{(2)}(k)$, as prolate as the prolate cycloid is self-intersecting and also it satisfies the condition $a < b$.

With the introduction of effective term, the properties of Hamiltonian changes, which are reflected in the curvature of parameter space. Based on the strength of the effective term, the parameter space curve behaves as a simple curve with non-closed, self-intersecting conditions.

For this BDI symmetry class, we have presented the curvature study of two different Hamiltonians. Hamiltonian $H^{(1)}(k)$ is the model Hamiltonian without effective term. In Hamiltonian $H^{(2)}(k)$, the effective term is added to the σ_y component. In both cases, the curvature is mirror symmetric about the κ -axis.

4.2 Results of AIII symmetry class

AIII symmetry is characterised by the absence of time-reversal and particle-hole symmetry. But it obeys chiral symmetry condition (figure 2). AIII symmetry class contains two Hamiltonians $H^{(3)}(k)$ and $H^{(4)}(k)$. Both Hamiltonians are topologically trivial in one dimension and satisfies all the symmetry properties.

4.2.1 $H^{(3)}(k)$ Hamiltonian. The matrix form of the Hamiltonian $H^{(3)}(k)$ is

$$\mathcal{H}^{(3)}(k)$$

$$= \begin{pmatrix} 2t \cos(k) + \mu + \delta_3 k & 2i \Delta \sin(k) \\ -2i \Delta \sin(k) & -2t \cos(k) - \mu - \delta_3 k \end{pmatrix}. \quad (37)$$

Here the set of possible parametric equations are

$$\begin{aligned} \chi^{(1)}(H^{(3)}(k)) &= 0 \\ \chi^{(2)}(H^{(3)}(k)) &= 2\Delta \sin k \\ \chi^{(3)}(H^{(3)}(k)) &= 2t \cos k + \mu + \delta_3 k. \end{aligned} \quad (38)$$

H_{BdG} Hamiltonian in the pseudospin basis is [41]

$$H^{(3)}(k) = \chi^{(2)}(H^{(3)}(k))\sigma_y + \chi^{(3)}(H^{(3)}(k))\sigma_z. \quad (39)$$

The energy dispersion relation

$$E^{(3)}(k) = \sqrt{(2t \cos k + \mu + \delta_3 k)^2 + (2\Delta \sin k)^2}.$$

The curvature of the Hamiltonian $H^{(3)}(k)$ is

$$\begin{aligned} \kappa(k) &= \frac{\det \begin{pmatrix} 2\Delta \cos k & -2\Delta \sin k \\ -2t \sin k + \delta_3 & -2t \cos k \end{pmatrix}}{\left(\sqrt{(-2t \sin k + \delta_3)^2 + 4\Delta^2 \cos^2 k} \right)^3} \\ &= \frac{-4t \Delta + 2\delta_3 \Delta \sin k}{\left(\sqrt{(2t \sin k + \delta_3)^2 + (2\alpha \cos k)^2} \right)^3}. \end{aligned} \quad (40)$$

Figure 4 consists of two panels for two different values of δ_3 . The upper and lower panels represent the parameter space $\delta_3 = 0.5$ and $\delta_3 = 1$ respectively. Each panel

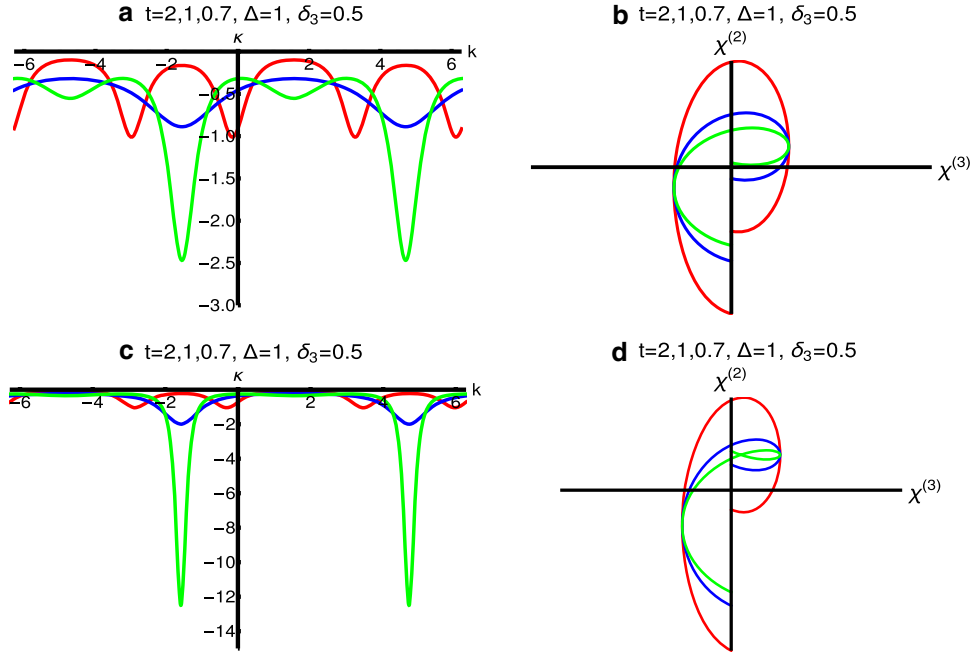


Figure 4. (a) Plots of curvature (κ) with k for $\delta_2 = 0.5$, (b) the corresponding parameter plots for the curvature plot (a), (c) plots of curvature (κ) with k for $\delta_2 = 1$ and (d) the corresponding parameter plots for the curvature plot (c). In all the plots, the red, blue and green curves represent $t = 2, 1, 0.7$ respectively.

consists of two plots, the left one is for curvature and the right one is for the corresponding parameter space curves. We observe that as the value of δ_3 increases, the curvature also increases.

It reveals in this study that the AIII symmetry class lacks the mirror symmetry about κ axis. As the value of δ_1 increases, the peaks become steep but their position is unaltered. As in the previous case, the curvature expression is independent of the term μ . The increase in the strength of the effective term results in a decrease of the curvature near $k = 0$. For the Hamiltonian $H^{(3)}(k)$, the parameter space curve is also a prolate cycloid because it is open self-intersecting.

From the curvature studies for this parameter space curve of Hamiltonian $H^{(3)}(k)$, it reveals that the curvature at the points $(-\pi$ and $\pi)$ on the semi-major axis is maximum and the curvature on the semi-minor axis is minimum. When the effective term changes its sign, the parameter space curves as well as curvature plots form mirror symmetric images [8].

4.2.2 $H^{(4)}(k)$ Hamiltonian. Hamiltonian $H^{(4)}(k)$ can be written in the matrix form as

$$\mathcal{H}^{(4)}(k) = \begin{pmatrix} 2t \cos(k) + \mu + \delta_3 k & 2i \Delta \sin(k) + i \delta_2 k \\ -2i \Delta \sin(k) - i \delta_2 k & -2t \cos(k) - \mu - \delta_3 k \end{pmatrix}. \quad (41)$$

Here the set of possible parametric equations are

$$\begin{aligned} \chi^{(1)}(H^{(4)}(k)) &= 0 \\ \chi^{(2)}(H^{(4)}(k)) &= 2\Delta \sin k + \delta_2 k, \\ \chi^{(3)}(H^{(4)}(k)) &= 2t \cos k + \mu + \delta_3 k. \end{aligned} \quad (42)$$

H_{BdG} Hamiltonian in the pseudospin basis is [41]

$$H(k)^{(4)} = \chi^{(2)}(H^{(4)}(k))\sigma_y + \chi^{(3)}(H^{(4)}(k))\sigma_z. \quad (43)$$

The energy dispersion relation

$$E^{(4)}(k) = \sqrt{(2\Delta \sin k + \delta_2 k)^2 + (2t \cos k + \mu + \delta_3 k)^2}.$$

The curvature is given by

$$\begin{aligned} \kappa(k) &= \frac{\text{Det} \begin{bmatrix} 2\Delta \cos k + \delta_2 & -2\Delta \sin k \\ -2t \sin k + \delta_3 & -2t \cos k \end{bmatrix}}{\left(\sqrt{(-2t \sin k + \delta_3)^2 + (2\Delta \cos k + \delta_2)^2}\right)^3} \\ &= \frac{-4t \Delta - 2(\delta_3 \Delta \sin k + \delta_2 t \cos k)}{\left(\sqrt{(-2t \sin k + \delta_3)^2 + (2\Delta \cos k + \delta_2)^2}\right)^3}. \end{aligned} \quad (44)$$

Equation (44) is an analytic expression of the curvature for the Hamiltonian $H^{(4)}(k)$.

Figure 5 consists of two panels for two different values of δ_2 and δ_3 . The upper and lower panels represent the parameter space $\delta_2 = 1, \delta_3 = 0.5$ and $\delta_2 = 0.5, \delta_3 = 1$ respectively. Each panel consists of two figures, the left one is for curvature and the right one is for the corresponding parameter space curves. We observe that with

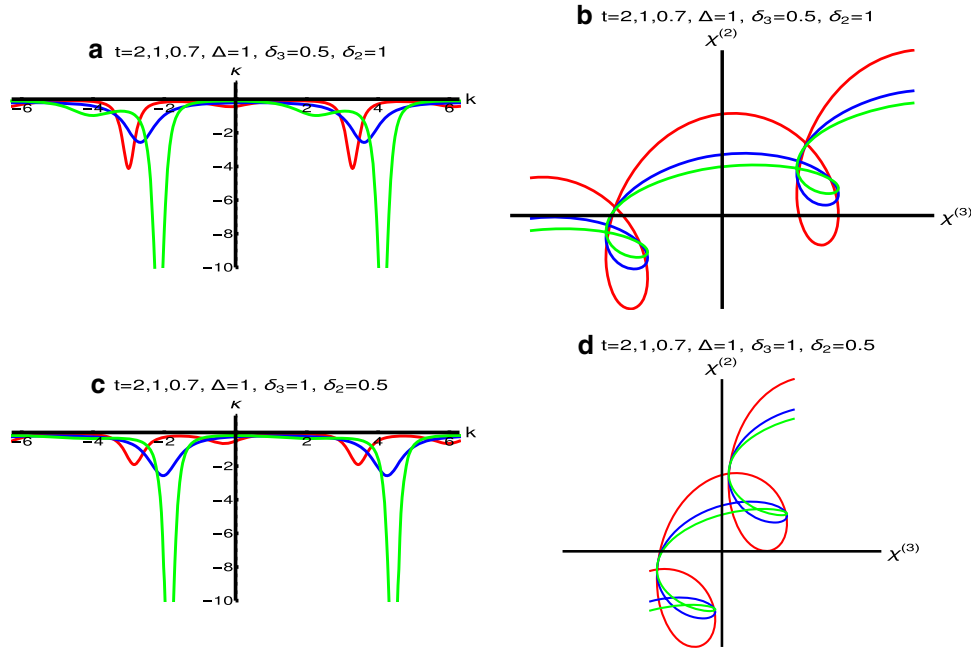


Figure 5. (a) Plots of curvature (κ) with k for $\delta_1 = 0.5$, (b) the corresponding parameter plots for the curvature plot (a), (c) plots of curvature (κ) with k for $\delta_2 = 0.5$ and (d) the corresponding parameter plots for the curvature plot (c). In all the plots, the red, blue and green curves represent $t = 2, 1, 0.7$ respectively.

increasing value of δ_2 , the curvature also increases. It clearly shows the evidence of divergence in the curvature plots. $H^{(4)}(k)$ shows that the asymmetry nature is the same as $H^{(3)}(k)$ Hamiltonian. For $H^{(4)}(k)$ Hamiltonian, parameter space curves form cycloidal pattern but in a very arbitrary way. There is no specific way of orientation. The corresponding curvature shows the non-topological state. Based on the strength of δ_2 and δ_3 , divergence characters arise at the BZ boundary values. The curvature plots show the divergence at BZ boundary regions, i.e., $-\pi$ and π .

In the AIII symmetry class, we have presented two model Hamiltonians. Hamiltonian $H^{(3)}(k)$ contains the effective term in the σ_z part and Hamiltonian $H^{(4)}(k)$ contains effective term both in the σ_y and σ_z components. Both of these Hamiltonians show distorted curves where curvature lacks mirror symmetry about the κ -axis.

Both BDI as well as AIII symmetry classes have distinct geometric properties. Through the curvature study, we can analyse the nature of parameter space, cycloidal motion of the parameter space with and without the addition of effective term. When the effective term is added to the σ_y or σ_z component of the Hamiltonian, the system remains in the \mathbf{R}^2 space and we observe only curvature. But the cycloidal motion of the \mathbf{R}^2 parameter space is nothing other than the helical motion in the \mathbf{R}^3 space. Hence, we consider the \mathbf{R}^3 space to investigate the torsional effect of effective term on the model Hamiltonian.

4.3 Results of A symmetry class

Symmetry class A is characterised by the absence of time-reversal (\mathcal{T}), particle-hole (\mathcal{C}) and chiral (\mathcal{S}) with the Hamiltonian 2. Here, the Hamiltonians $H^{(5)}(k)$, $H^{(6)}(k)$, $H^{(7)}(k)$ and $H^{(8)}(k)$ belong to the A class [8]. These Hamiltonians show topologically trivial behaviour for a one-dimensional system.

4.3.1 $H^{(5)}(k)$ Hamiltonian. Hamiltonian $H^{(5)}(k)$ can be written in the matrix form as

$$\mathcal{H}^{(5)}(k) = \begin{pmatrix} 2t \cos(k) + \mu & 2i \Delta \sin(k) + \delta_1 k \\ -2i \Delta \sin(k) + \delta_1 k & 2t \cos(k) + \mu \end{pmatrix}. \quad (45)$$

Here the set of possible parametric equations are

$$\begin{aligned} \chi^{(1)}(H^{(5)}(k)) &= \delta_1 k, \\ \chi^{(2)}(H^{(5)}(k)) &= 2\Delta \sin k, \\ \chi^{(3)}(H^{(5)}(k)) &= 2t \cos k + \mu. \end{aligned} \quad (46)$$

H_{BaG} Hamiltonian in the pseudospin basis is [41]

$$\begin{aligned} H(k)^{(5)} &= \chi^{(1)}(H^{(5)}(k))\sigma_x + \chi^{(2)}(H^{(5)}(k))\sigma_y \\ &\quad + \chi^{(3)}(H^{(5)}(k))\sigma_z. \end{aligned} \quad (47)$$

The energy dispersion relation

$$E^{(5)}(k) = \sqrt{(\delta_1 k)^2 + (2\Delta \sin k)^2 + (-2t \cos k - \mu)^2}.$$

The parameter space of $H^{(5)}(k)$ belongs to \mathbf{R}^3 space and forms the circular helix as

$$\text{helix } [a, b](k) = (a \cos(k), a \sin(k), bk), \quad (48)$$

where a is the radius and b is the slope of the helix (here for all the cases we take $\Delta = t$ to achieve unit speed curve properties). The projection of \mathbf{R}^3 onto \mathbf{R}^2 maps the helix onto a circle.

Here the curve is

$$c(k) = \begin{bmatrix} \delta_1 k \\ 2\Delta \sin k \\ 2t \cos k + \mu \end{bmatrix}, \quad \dot{c}(k) = \begin{bmatrix} \delta_1 \\ 2\Delta \cos k \\ -2t \sin k \end{bmatrix},$$

$$\ddot{c}(k) = \begin{bmatrix} 0 \\ -2\Delta \sin k \\ -2t \cos k \end{bmatrix} \quad (49)$$

and thus the curvature $\kappa = \|\ddot{c}(k)\| = 2$ which represents the non-vanishing curvature. Hence, it is possible to find normal vector for all values of k . Thus,

$$n(k) = \frac{\ddot{c}(k)}{\kappa(k)} = \frac{1}{2} \begin{bmatrix} 0 \\ -2\Delta \sin k \\ -2t \cos k \end{bmatrix}. \quad (50)$$

$$\mathcal{H}^{(6)}(k) = \begin{pmatrix} 2t \cos(k) + \mu & 2i \Delta \sin(k) + i\delta_2 k + \delta_1 k \\ -2i \Delta \sin(k) - i\delta_2 k + \delta_1 k & 2t \cos(k) + \mu \end{pmatrix}. \quad (54)$$

Bi-normal vector is given by

$$b(k) = \dot{c} \times n(k) = \begin{bmatrix} \delta_1 \\ 2\Delta \cos k \\ -2t \sin k \end{bmatrix} \times \frac{1}{2} \begin{bmatrix} 0 \\ -2\Delta \sin k \\ -2t \cos k \end{bmatrix}$$

$$= \frac{1}{2} \begin{bmatrix} -4t \Delta \\ -2\Delta \delta_1 \sin k \\ -2t \delta_1 \cos k \end{bmatrix}. \quad (51)$$

The torsion is given by

$$\langle \dot{n}(k), b(k) \rangle = \left\langle \frac{1}{2} \begin{bmatrix} 0 \\ -2\Delta \cos k \\ 2t \sin k \end{bmatrix}, \frac{1}{2} \begin{bmatrix} -4t \Delta \\ -2\Delta \delta_1 \sin k \\ -2t \delta_1 \cos k \end{bmatrix} \right\rangle$$

$$= t \Delta \delta_1. \quad (52)$$

Thus, the curvature as well as the torsion give constant values for $H^{(5)}(k)$.

Serret–Frenet equation (eq. (24)) for $H^{(5)}(k)$ Hamiltonian is

$$\dot{T}(k) = \begin{bmatrix} 0 \\ -2\Delta \sin k \\ -2t \cos k \end{bmatrix},$$

$$\dot{N}(k) = -2 \begin{bmatrix} \delta_1 \\ 2\Delta \cos k \\ -2t \sin k \end{bmatrix} + \frac{t \Delta \delta_1}{2} \begin{bmatrix} -4t \Delta \\ -2\Delta \delta_1 \sin k \\ -2t \delta_1 \cos k \end{bmatrix},$$

$$\dot{B}(k) = -\frac{t \Delta \delta_1}{2} \begin{bmatrix} 0 \\ -2\Delta \sin k \\ -2t \cos k \end{bmatrix}. \quad (53)$$

Serret–Frenet equation (eq. (24)) for the Hamiltonian $H^{(5)}(k)$ gives the understanding about the dynamics of $H^{(5)}(k)$ Hamiltonian. When the $H^{(5)}(k)$ Hamiltonian is projected from $\mathbf{R}^3 \rightarrow \mathbf{R}^2$, one can obtain the $H^{(1)}(k)$ Hamiltonian.

Figure 6 shows the study of curvature as well torsion to $H^{(5)}(k)$ Hamiltonian. The left panel indicates the parameter space and the right panel indicates the corresponding curvature and torsion for different values of δ_1 . From the plot it is clear that, by increasing the values of δ_1 , the amplitude of curvature and torsion also increase. Hence, the curvature and torsion are directly proportional to δ_1 .

4.3.2 $H^{(6)}(k)$ Hamiltonian. Hamiltonian $H^{(6)}(k)$ can be written in the matrix form as

Here the set of possible parametric equations are

$$\chi^{(1)}(H^{(6)}(k)) = \delta_1 k,$$

$$\chi^{(2)}(H^{(6)}(k)) = 2\Delta \sin k + \delta_2 k,$$

$$\chi^{(3)}(H^{(6)}(k)) = 2t \cos k + \mu. \quad (55)$$

H_{BdG} Hamiltonian in the pseudospin basis is [41]

$$H(k)^{(6)} = \chi^{(1)}(H^{(6)}(k))\sigma_x + \chi^{(2)}(H^{(6)}(k))\sigma_y$$

$$+ \chi^{(3)}(H^{(6)}(k))\sigma_z. \quad (56)$$

The energy dispersion relation

$$E^{(6)}(k) = \sqrt{(\delta_1 k)^2 + (2\Delta \sin k + \delta_2 k)^2 + (-2t \cos k - \mu)^2}.$$

Here the curve is

$$c(k) = \begin{bmatrix} \delta_1 k \\ 2\Delta \sin k + \delta_2 k \\ 2t \cos k + \mu \end{bmatrix}, \quad \dot{c}(k) = \begin{bmatrix} \delta_1 \\ 2\Delta \cos k + \delta_2 \\ -2t \sin k \end{bmatrix},$$

$$\ddot{c}(k) = \begin{bmatrix} 0 \\ -2\Delta \sin k \\ -2t \cos k \end{bmatrix} \quad (57)$$

and thus the curvature $\kappa = \|\ddot{c}(k)\| = 2$ which represents the non-vanishing curvature. Hence, it is possible

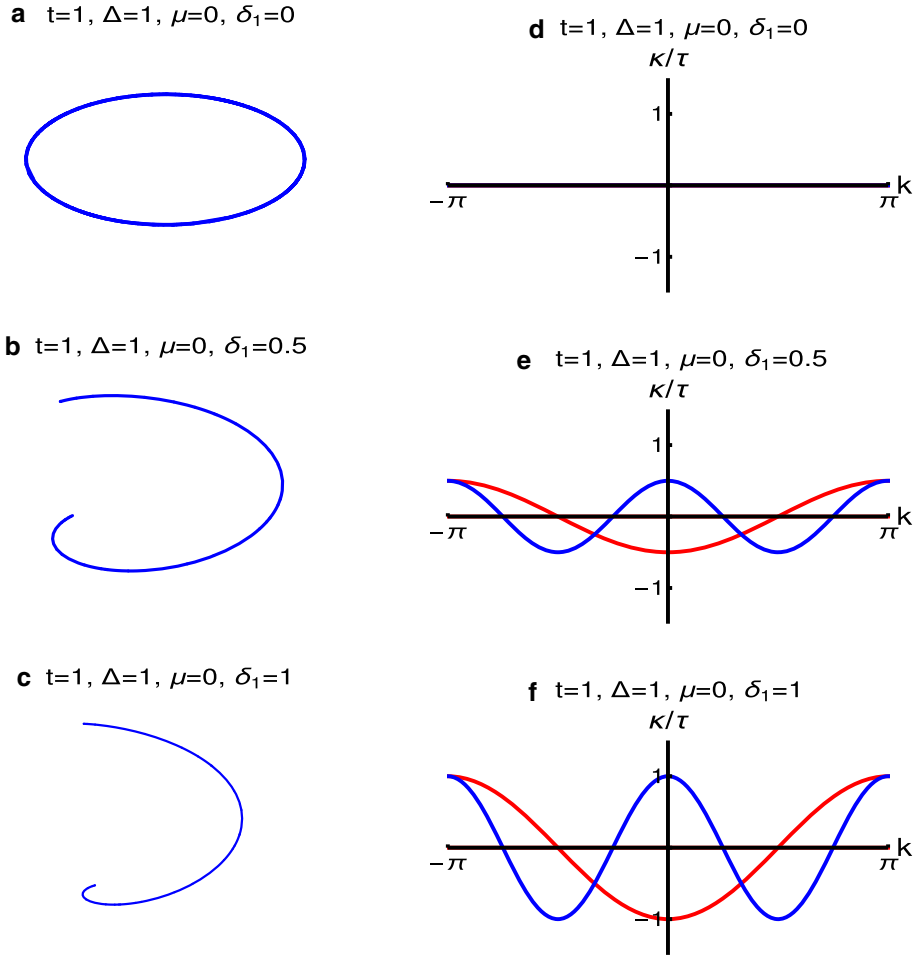


Figure 6. (Left) Parameter plots for the Hamiltonian $H^{(5)}(k)$. (Right) Plots of curvature (κ) and torsion (τ) with k for $t = \Delta = 1$ and $\alpha = 0, 0.5$ and 1 . The red and blue lines in the right panel represent the corresponding normal curvatures and torsion respectively.

to find normal vector for all values of k . Thus,

$$n(k) = \frac{\ddot{c}(k)}{\kappa(k)} = \frac{1}{2} \begin{bmatrix} 0 \\ -2\Delta \sin k \\ -2t \cos k \end{bmatrix}.$$

Bi-normal vector is given by

$$b(k) = \dot{c} \times n(k) = \begin{bmatrix} \delta_1 \\ 2\Delta \cos k + \delta_2 \\ -2t \sin k \end{bmatrix} \times \frac{1}{2} \begin{bmatrix} 0 \\ -2\Delta \sin k \\ -2t \cos k \end{bmatrix} = \frac{1}{2} \begin{bmatrix} -4t\Delta - 2t\delta_2 \cos k \\ -2\Delta\delta_1 \sin k \\ -2t\delta_1 \cos k \end{bmatrix}.$$

The torsion is given by

$$\langle \dot{n}(k), b(k) \rangle$$

$$= \left\langle \frac{1}{2} \begin{bmatrix} 0 \\ -2\Delta \cos k \\ 2t \sin k \end{bmatrix}, \frac{1}{2} \begin{bmatrix} -4t\Delta - 2t\delta_2 \cos k \\ -2\Delta\delta_1 \sin k \\ -2t\delta_1 \cos k \end{bmatrix} \right\rangle = t\Delta\delta_1. \tag{58} \tag{60}$$

Thus, the curvature as well as the torsion give constant values for $H^{(6)}(k)$. Serret–Frenet equation (eq. (24)) for the Hamiltonian $H^{(6)}(k)$ can be written as

$$\begin{aligned} \dot{T}(k) &= \begin{bmatrix} 0 \\ -2\Delta \sin k \\ -2t \cos k \end{bmatrix}, \\ \dot{N}(k) &= -2 \begin{bmatrix} \delta_1 \\ 2\Delta \cos k + \delta_2 \\ -2t \sin k \end{bmatrix} \\ &\quad + \frac{t\Delta\delta_1}{2} \begin{bmatrix} -4t\Delta - 2t\delta_2 \cos k \\ -2\Delta\delta_1 \sin k \\ -2t\delta_1 \cos k \end{bmatrix}, \end{aligned}$$

$$\dot{B}(k) = -\frac{t\Delta\delta_1}{2} \begin{bmatrix} 0 \\ -2\Delta \sin k \\ -2t \cos k \end{bmatrix}. \tag{61}$$

Thus, Serret–Frenet equation for the Hamiltonian $H^{(6)}(k)$ gives an understanding about the dynamics of $H^{(6)}(k)$ Hamiltonian. When the $H^{(6)}(k)$ Hamiltonian is projected from $\mathbf{R}^3 \rightarrow \mathbf{R}^2$, one can obtain the $H^{(2)}(k)$ Hamiltonian.

4.3.3 $H^{(7)}(k)$ Hamiltonian. Hamiltonian $H^{(7)}(k)$ can be written in the matrix form as

$$\mathcal{H}^{(7)}(k) = \begin{pmatrix} 2t \cos(k) + \mu + \delta_3 k & 2i \Delta \sin(k) + \delta_1 k \\ -2i \Delta \sin(k) + \delta_1 k & -2t \cos(k) - \mu - \delta_3 k \end{pmatrix}. \tag{62}$$

Here the set of possible parametric equations are

$$\begin{aligned} \chi^{(1)}(H^{(7)}(k)) &= \delta_1 k, \\ \chi^{(2)}(H^{(7)}(k)) &= 2\Delta \sin k, \\ \chi^{(3)}(H^{(7)}(k)) &= 2t \cos k + \mu + \delta_3 k. \end{aligned} \tag{63}$$

H_{BdG} Hamiltonian in the pseudospin basis is [41]

$$H(k)^{(7)} = \chi^{(1)}(H^{(7)}(k))\sigma_x + \chi^{(2)}(H^{(7)}(k))\sigma_y + \chi^{(3)}(H^{(7)}(k))\sigma_z. \tag{64}$$

The energy dispersion relation

$$E^{(7)}(k) = \sqrt{(\delta_1 k)^2 + (2\Delta \sin k)^2 + (2t \cos k + \mu + \delta_3 k)^2}.$$

Here, the curve is

$$\begin{aligned} c(k) &= \begin{bmatrix} \delta_1 k \\ 2\Delta \sin k \\ 2t \cos k + \mu + \delta_3 k \end{bmatrix}, \\ \dot{c}(k) &= \begin{bmatrix} \delta_1 \\ 2\Delta \cos k \\ -2t \sin k + \delta_3 \end{bmatrix}, \\ \ddot{c}(k) &= \begin{bmatrix} 0 \\ -2\Delta \sin k \\ -2t \cos k \end{bmatrix} \end{aligned} \tag{65}$$

and thus the curvature $\kappa = \|\ddot{c}(k)\| = 2$ which represents the non-vanishing curvature. Hence, it is possible to find normal vector for all values of k . Thus,

$$n(k) = \frac{\ddot{c}(k)}{\kappa(k)} = \frac{1}{2} \begin{bmatrix} 0 \\ -2\Delta \sin k \\ -2t \cos k \end{bmatrix}. \tag{66}$$

Bi-normal vector is given by

$$\begin{aligned} b(k) = \dot{c} \times n(k) &= \begin{bmatrix} \delta_1 \\ 2\Delta \cos k \\ -2t \sin k + \delta_3 \end{bmatrix} \\ &\times \frac{1}{2} \begin{bmatrix} 0 \\ -2\Delta \sin k \\ -2t \cos k \end{bmatrix} \\ &= \frac{1}{2} \begin{bmatrix} -4t\Delta - 2\Delta\delta_3 \sin k \\ -2\Delta\delta_1 \sin k \\ -2t\delta_1 \cos k \end{bmatrix}. \end{aligned} \tag{67}$$

The torsion is given by

$$\begin{aligned} \langle \dot{n}(k), b(k) \rangle &= \left\langle \frac{1}{2} \begin{bmatrix} 0 \\ -2\Delta \cos k \\ 2t \sin k \end{bmatrix}, \frac{1}{2} \begin{bmatrix} -4t\Delta - 2\Delta\delta_3 \sin k \\ -2\Delta\delta_1 \sin k \\ -2t\delta_1 \cos k \end{bmatrix} \right\rangle \\ &= t\Delta\delta_1. \end{aligned} \tag{68}$$

Thus, the curvature as well as the torsion give constant values for $H^{(7)}(k)$. Serret–Frenet equation (eq. (24)) for the Hamiltonian $H^{(7)}(k)$ can be written as

$$\begin{aligned} \dot{T}(k) &= \begin{bmatrix} 0 \\ -2\Delta \sin k \\ -2t \cos k \end{bmatrix}, \\ \dot{N}(k) &= -2 \begin{bmatrix} \delta_1 \\ 2\Delta \cos k \\ -2t \sin k + \delta_3 \end{bmatrix} \\ &+ \frac{t\Delta\delta_1}{2} \begin{bmatrix} -4t\Delta - 2\Delta\delta_3 \sin k \\ -2\Delta\delta_1 \sin k \\ -2t\delta_1 \cos k \end{bmatrix}, \\ \dot{B}(k) &= -\frac{t\Delta\delta_1}{2} \begin{bmatrix} 0 \\ -2\Delta \sin k \\ -2t \cos k \end{bmatrix}. \end{aligned} \tag{69}$$

Thu, Serret–Frenet equation for the Hamiltonian $H^{(7)}(k)$ gives an understanding about the dynamics of $H^{(7)}(k)$ Hamiltonian. When the $H^{(7)}(k)$ Hamiltonian is projected from $\mathbf{R}^3 \rightarrow \mathbf{R}^2$, one can obtain the $H^{(3)}(k)$ Hamiltonian.

4.3.4 $H^{(8)}(k)$ Hamiltonian. Hamiltonian $H^{(8)}(k)$ can be written in the matrix form as

$$\begin{aligned} \mathcal{H}^{(8)}(k) &= \begin{pmatrix} 2t \cos(k) + \mu + \delta_3 k & 2i \Delta \sin(k) + i\delta_2 k \\ -2i \Delta \sin(k) + \delta_1 k & 2t \cos(k) + \mu + \delta_3 k \end{pmatrix} \\ &= \begin{pmatrix} 2t \cos(k) + \mu + \delta_3 k & 2i \Delta \sin(k) + i\delta_2 k \\ -2i \Delta \sin(k) + \delta_1 k & 2t \cos(k) + \mu + \delta_3 k \end{pmatrix}. \end{aligned} \tag{70}$$

Here the set of possible parametric equations are

$$\begin{aligned}\chi^{(1)}(H^{(8)}(k)) &= \delta_1 k, \\ \chi^{(2)}(H^{(8)}(k)) &= 2\Delta \sin k + \delta_2 k, \\ \chi^{(3)}(H^{(8)}(k)) &= 2t \cos k + \mu + \delta_3 k.\end{aligned}\quad (71)$$

H_{BdG} Hamiltonian in the pseudospin basis is [41]

$$H(k)^{(8)} = \chi^{(1)}(H^{(8)}(k))\sigma_x + \chi^{(2)}(H^{(8)}(k))\sigma_y + \chi^{(3)}(H^{(8)}(k))\sigma_z.\quad (72)$$

The energy dispersion relation

$$E^{(8)}(k) = \sqrt{(\delta_1 k)^2 + (2\Delta \sin k + \delta_2 k)^2 + (2t \cos k + \mu + \delta_3 k)^2}.$$

Here the curve is

$$\begin{aligned}c(k) &= \begin{bmatrix} \delta_1 k \\ 2\Delta \sin k + \delta_2 k \\ 2t \cos k + \mu + \delta_3 k \end{bmatrix}, \\ \dot{c}(k) &= \begin{bmatrix} \delta_1 \\ 2\Delta \cos k + \delta_2 \\ -2t \sin k + \delta_3 \end{bmatrix}, \\ \ddot{c}(k) &= \begin{bmatrix} 0 \\ -2\Delta \sin k \\ -2t \cos k \end{bmatrix}\end{aligned}\quad (73)$$

and thus the curvature $\kappa = \|\ddot{c}(k)\| = 2$ which represents the non-vanishing curvature. Hence, it is possible to find normal vector for all values of k . Thus,

$$n(k) = \frac{\ddot{c}(k)}{\kappa(k)} = \frac{1}{2} \begin{bmatrix} 0 \\ -2\Delta \sin k \\ -2t \cos k \end{bmatrix}.\quad (74)$$

Bi-normal vector is given by

$$\begin{aligned}b(k) &= \dot{c} \times n(k) = \begin{bmatrix} \delta_1 \\ 2\Delta \cos k + \delta_2 \\ -2t \sin k + \delta_3 \end{bmatrix} \\ &\quad \times \frac{1}{2} \begin{bmatrix} 0 \\ -2\Delta \sin k \\ -2t \cos k \end{bmatrix} \\ &= \frac{1}{2} \begin{bmatrix} -4t\Delta - 2t\delta_2 \cos k - 2\Delta\delta_3 \sin k \\ -2\Delta\delta_1 \sin k \\ -2t\delta_1 \cos k \end{bmatrix}.\end{aligned}\quad (75)$$

The torsion is given by

$$\begin{aligned}\langle \dot{n}(k), b(k) \rangle &= \left\langle \frac{1}{2} \begin{bmatrix} 0 \\ -2\Delta \cos k \\ 2t \sin k \end{bmatrix}, \frac{1}{2} \begin{bmatrix} -4t\Delta - 2t\delta_2 \cos k - 2\Delta\delta_3 \sin k \\ -2\Delta\delta_1 \sin k \\ -2t\delta_1 \cos k \end{bmatrix} \right\rangle \\ &= t\Delta\delta_1.\end{aligned}\quad (76)$$

Thus, the curvature as well as the torsion give constant values for $H^{(8)}(k)$. By using eq. (24), Serret–Frenet equation for the $H^{(8)}(k)$ Hamiltonian can be written as

$$\begin{aligned}\dot{T}(k) &= \begin{bmatrix} 0 \\ -2\Delta \sin k \\ -2t \cos k \end{bmatrix}, \\ \dot{N}(k) &= -2 \begin{bmatrix} \delta_1 \\ 2\Delta \cos k + \delta_2 \\ -2t \sin k + \delta_3 \end{bmatrix}\end{aligned}$$

$$\begin{aligned}\dot{B}(k) &= \frac{t\Delta\delta_1}{2} \begin{bmatrix} -4t\Delta - 2t\delta_2 \cos k - 2\Delta\delta_3 \sin k \\ -2\Delta\delta_1 \sin k \\ -2t\delta_1 \cos k \end{bmatrix}, \\ &\quad - \frac{t\Delta\delta_1}{2} \begin{bmatrix} 0 \\ -2\Delta \sin k \\ -2t \cos k \end{bmatrix}.\end{aligned}\quad (77)$$

Thus, Serret–Frenet equation for the $H^{(8)}(k)$ Hamiltonian gives an understanding about the dynamics of the $H^{(8)}(k)$ Hamiltonian. When the $H^{(8)}(k)$ Hamiltonian is projected from $\mathbf{R}^3 \rightarrow \mathbf{R}^2$, one can obtain the $H^{(4)}(k)$ Hamiltonian.

Thus, it is very clear that the projection of $\mathbf{R}^3 \rightarrow \mathbf{R}^2$ space ($\chi_2 - \chi_3$ parameter space) signals the changes in the geometrical properties of the model Hamiltonian. In the \mathbf{R}^3 space, the Hamiltonian belongs to the symmetry class A, but when it is projected to \mathbf{R}^2 space, it belongs to either BDI or AIII symmetry class. It is a very important point that, under the given conditions, Hamiltonians belonging to the symmetry class A show the same curvature and torsion. But the Hamiltonians belonging to BDI and AIII symmetry classes have different curvature expressions.

4.4 Geodesic properties of the curve for $H^{(5)}(k)$ Hamiltonian

Geodesics are the shortest path between two points in a surface. Geodesics always have a constant speed. Sometimes geodesics can be expressed as geodesic curvature (k_g). Hence, as a part of curvature study, we consider

a unit-speed curve on a circular cylinder which actually forms a helix on the surface. It is interesting that at the intersection of a cylinder, the plane perpendicular to its rulings is always a geodesic. Here we consider $H^{(5)}(k)$ Hamiltonian and calculate the geodesic by geometrical operations.

Local isometry is the quantity which can give a clear understanding about this. For a unit cylinder W with the conditions $x^2 + y^2 = 1$, there always exists geodesic with the circles obtained by intersecting W with planes parallel to the x - y plane. Because of the local isometric property, one can connect the points $(u, v, 0)$ of the x - y plane to the points $(\cos u, \sin u, v)$ of the W plane. This makes a geodesic from x - y plane to the geodesic on W . The line which is not parallel to the y -axis in the x - y plane gives the equation $y = mx + c$, where m and c are constants. Parametrising the line by $x = k$ and $y = mk + c$ we get $c(k) = (\cos(k), \sin(k), mk + c)$ which is nothing other than the similar helix considered in $H^{(5)}(k)$. Here we clearly give the geodesic curve for $H^{(5)}(k)$. Let there be a circular cylinder,

$$W = \{X = (\chi_1, \chi_2, \chi_3) \in R^3 | \chi_2^2 + \chi_3^2 = 1, \chi_1 = k, k \in R\}. \tag{78}$$

Here, we consider $H^{(5)}(k)$ Hamiltonian with the condition $\mu = 0, t = \Delta = 1/2$ and $\delta_1 = 1$. The minimum condition for a curve $c: I \rightarrow W$ on W to be a geodesic is that the curve $c(k)$ should be inclined on W . Let the curve $c(k)$ be a geodesic on the circular cylinder W .

Now

$$\dot{c}(k) = \frac{dc}{dk} = V_1.$$

If the angle between V_1 and $d/d\chi_3$ is $\phi(k)$, then for every k [42],

$$\left\langle V_1, \frac{d}{d\chi_1} = \cos(\phi(k)) \right\rangle. \tag{79}$$

By taking covariant derivatives with respect to V_1

$$\left\langle D_{V_1} V_1, \frac{d}{d\chi_1} \right\rangle + \left\langle V_1 D_{V_1}, \frac{d}{d\chi_1} \right\rangle = -\sin(\phi(k)) \frac{d\phi}{dk} \tag{80}$$

or in other words

$$\left\langle k_1 V_2, \frac{d}{d\chi_1} \right\rangle = -\sin(\phi(k)) \frac{d\phi}{dk}, \tag{81}$$

where

$$V_2 = \frac{\ddot{c}(k)}{\|\ddot{c}(k)\|}, \quad \|\ddot{c}(k)\| = k_1.$$

Then

$$\left\langle \ddot{c}, \frac{d}{d\chi_1} \right\rangle = -\sin(\phi(k)) \frac{d\phi}{dk}.$$

Here the curve $c(k)$ is a unit speed curve (under given conditions) and a geodesic on the circular helical. Hence, we get $\ddot{c}(k) = \lambda N$. For a N vector area defined by $N_p = (p_1, p_2, p_3, \dots, p_{n-1} = 0)$ for $p = (p_1, p_2, \dots, p_n) \in W$ is the unit normal vector area of W . So,

$$\left\langle N, \frac{\partial_n}{\partial k_n} \right\rangle = \sin(\phi(k)) \frac{d\phi}{dk} = 0. \tag{82}$$

Now

$$\sin(\phi(k)) = 0 \quad \text{or} \quad \frac{d\phi(k)}{dk} = 0.$$

So

$$\frac{d\phi(k)}{dk} = 0 \implies \phi(k) = 0 \quad \text{or} \quad \phi(k) = \text{constant}.$$

This shows that the curve is an inclined curve with $d/d\chi_1$ as the axis on the circular cylinder W .

In other words,

$$\left\langle V_1, \frac{dV_1}{d\chi_1} \right\rangle = \cos(\phi(k)), \quad \phi(k) \neq \pi/2 (\phi = \text{constant}). \tag{83}$$

Hence,

$$\left\langle k_1 V_2, \frac{d}{d\chi_1} \right\rangle = 0.$$

The covariant derivative with respect to V_1 is

$$\left\langle \frac{dV_1}{dk}, \frac{d}{d\chi_1} \right\rangle = 0 \implies \left\langle N, \frac{d}{d\chi_1} \right\rangle = 0. \tag{84}$$

It shows $\langle \ddot{c}(k), \dot{c}(k) \rangle = 0$ and $N, \dot{c}(k) = 0$, where

$$N = \lambda \frac{d}{d\chi_1} \wedge \dot{c}(k) \\ \ddot{c} = \beta \frac{d}{d\chi_1} \wedge \dot{c}(k). \tag{85}$$

Then $\ddot{c}(k) = \beta N$, which clearly shows that the inclined curve is a geodesic under a given parameter space.

Here, we consider just $H^{(5)}(k)$ Hamiltonian under some particular parameter space to calculate the geodesics. We choose the parameter space in such a way that the curve $c(k)$ remains unit-speed. In other Hamiltonians, it is not possible to achieve unit-speed curve. And we consider unit cylinder with the condition $x^2 + y^2 = 1$. This case is only possible in $H^{(5)}(k)$ Hamiltonian. When the effective term is added to either σ_y or σ_z , the curve fails to be a unit-speed curve. As this condition is not possible in other Hamiltonians, we only calculate geodesic curvature for $H^{(5)}(k)$ Hamiltonian.

4.5 Consequences of effective term and its physical interpretation

The differential geometric analysis of the parameter space makes us understand the nature of Hamiltonians of different symmetry classes. This effort successfully explains the curvature study of the parameter space with the addition of effective term αk and the transition of system from topological to topologically trivial phase. Curvature and torsion are integral parts of a geometrical system and one can understand the physical system in a better way by this study. In the study of space–time geometry, mass is responsible for curvature and spin is responsible for torsion [25]. In the same way, for our present model, the dependence of momentum vector k in terms ‘sine’ and ‘cosine’ is responsible for the curvature and effective term αk is responsible for the torsional effects. The cycloidal motion in a \mathbf{R}^2 space is a cycloid when it is projected to a \mathbf{R}^3 space and a unit-speed cycloid in a \mathbf{R}^3 space is a unit-speed circle when it is projected to a \mathbf{R}^2 space. This helps us to understand the relation between the geometry and physics of a quantum condensed matter system.

When the same analogy is applied to a lattice model, the initial Hamiltonian $H_0(k)$ represents a tight-binding model and the effective term $\delta_i k$ represents the external interaction term which is linear momentum (in some cases it is similar to magnetic field). Because of the nature of the effective term, it gives rise to torsion in the lattice system. So it results in the curve opening of parameter space and cycloidal motion.

For the tight-binding models, this type of torsion results in dislocations and disclinations [25]. It is similar to the disorder and defect in the crystal lattices. In our Hamiltonians, the periodicity of the Bloch space breaks and the system transforms from topological to non-topological phase. This transformation is the result of torsion. Even though the system transforms from topological to trivial phase, the model remains in the respective symmetry classes (BDI, AIII and A).

5. Conclusion

We have presented entirely new and insightful results of curvature analysis for different symmetry classes, each system class containing different Hamiltonians with different topological properties. We have shown explicitly the merits and limitations of curvature study in the presence of effective term. We have analysed the behaviour of the system from topological to non-topological state with the addition of effective term to the model Hamiltonian. We have shown explicitly the presence of mirror symmetry for the curvature study of BDI symmetry

class but that symmetries are absent for the AIII and A symmetry classes. We have introduced the concept of torsion in topological state of matter, thereby explained the transformation of the system from topological to non-topological state and we observed a transformation of symmetry classes, when there is a projection from \mathbf{R}^3 space to \mathbf{R}^2 space. We have given the geodesic properties of certain Hamiltonian under given conditions. This work provides a new perspective on the curvature analysis for the topological state of matter.

Acknowledgements

SS would like to acknowledge DST (EMR/2017/000898) for the funding and RRI library for the books and journals. YRK would like to thank Admar Mutt Education Foundation for the scholarship. The authors would like to acknowledge Dr R Srikanth, Dr B S Ramachandra and Prof. C Sivaram for reading this manuscript critically and for giving useful suggestions. This research was supported in part by the International Centre for Theoretical Sciences (ICTS) during a visit for participating in the program – Geometry and Topology for Lecturers (Code: ICTS/gtl2018/06).

References

- [1] C-K Chiu, J C Y Teo, A P Schnyder and S Ryu, *Rev. Mod. Phys.* **88**(3), 035005 (2016)
- [2] M Z Hasan and C L Kane, *Rev. Mod. Phys.* **82**(4), 3045 (2010)
- [3] M Sato and Y Ando, *Rep. Prog. Phys.* **80**(7), 076501 (2017)
- [4] A Altland and M R Zirnbauer, *Phys. Rev. B* **55**(2), 1142 (1997)
- [5] T D Stanescu, *Introduction to topological quantum matter & quantum computation* (CRC Press, 2016)
- [6] T Senthil, *Annu. Rev. Condens. Matter Phys.* **6**(1), 299 (2015)
- [7] B A Bernevig and T L Hughes, *Topological insulators and topological superconductors* (Princeton University Press, 2013)
- [8] S Rahul, R Ranjith Kumar, Y R Kartik, A Banerjee and S Sarkar, *Phys. Scr.* **94**(11), 115803 (2019)
- [9] R Ranjith Kumar and S Sarkar, *Phase Transit.* **93**(3), (2020)
- [10] C G Velasco and B Paredes, [arXiv:1907.11460](https://arxiv.org/abs/1907.11460) (2019)
- [11] S Sarkar, *Sci. Rep.* **8**(1), 5864 (2018)
- [12] V A Toponogov, *Differential geometry of curves and surfaces* (Springer, 2006)
- [13] C Bär, *Elementary differential geometry* (Cambridge University Press, 2010)

- [14] E Abbena, S Salamon and A Gray, *Modern differential geometry of curves and surfaces with Mathematica* (Chapman and Hall/CRC, 2017)
- [15] S M Carroll, *Spacetime and geometry. An introduction to general relativity* (2004)
- [16] B F Schutz, *Geometrical methods of mathematical physics* (Cambridge University Press, 1980)
- [17] B Schutz, *A first course in general relativity* (Cambridge University Press, 2009)
- [18] D-J Zhang, Q-h Wang and J Gong, [arXiv:1811.04640](https://arxiv.org/abs/1811.04640) (2018)
- [19] A N Pressley, *Elementary differential geometry* (Springer Science & Business Media, 2010)
- [20] P M H Wilson, *Curved spaces: From classical geometries to elementary differential geometry* (Cambridge University Press, 2007)
- [21] Y Mokrousov and F Freimuth, [arXiv:1407.2847](https://arxiv.org/abs/1407.2847) (2014)
- [22] S Montiel and A Ros, *Curves and surfaces* (American Mathematical Soc., 2009) Vol. 69
- [23] D D Sheka, V P Kravchuk, K V Yershov and Y Gaididei, *Phys. Rev. B* **92(5)**, 054417 (2015)
- [24] A A Lima, C Filgueiras and F Moraes, *Eur. Phys. J. B* **90(2)**, 32 (2017)
- [25] V D Sabbata and C Sivaram, *Spin and torsion in gravitation* (World Scientific, 1994)
- [26] T L Hughes, R G Leigh and O Parrikar, *Phys. Rev. D* **88(2)**, 025040 (2013)
- [27] Z V Khaidukov and M A Zubkov, *JETP Lett.* **108(10)**, (2018)
- [28] M Kolodrubetz, V Gritsev and A Polkovnikov, *Phys. Rev. B* **88(6)**, 064304 (2013)
- [29] P R Zulkowski, D A Sivak, G E Crooks and M R DeWeese, *Phys. Rev. E* **86(4)**, 041148 (2012)
- [30] M Lakshmanan, *Philos. Trans. R. Soc. A* **369(1939)**, 1280 (2011)
- [31] M Lakshmanan, Th W Ruijgrok and C J Thompson, *Physica A* **84(3)**, 577 (1976)
- [32] M Lakshmanan, *Phys. Lett. A* **61(1)**, 53 (1977)
- [33] I M Georgescu, S Ashhab and F Nori, *Rev. Mod. Phys.* **86(1)**, (2014)
- [34] S Sarkar, *EPL* **110(6)**, (2015)
- [35] S Sarkar, *Physica B Condens. Matter* **475**, (2015)
- [36] A Y Kitaev, *Phys-USP* **44(10S)**, 131 (2001)
- [37] M V Berry, *J. Phys. A* **18(1)**, 15 (1985)
- [38] M J Ablowitz and A S Fokas, *Complex variables: Introduction and applications* (Cambridge University Press, 2003)
- [39] P Kotetes, *Topological insulators and superconductors-Notes of TKMI 2013/2014 guest lectures*
- [40] K Shiozaki and M Sato, *Phys. Rev. B* **90(16)**, 165114 (2014)
- [41] Y Niu, S B Chung, C-H Hsu, I Mandal, S Raghu and S Chakravarty, *Phys. Rev. B* **85(3)**, 035110 (2012)
- [42] G K Yücekaya and H H Hacısalihoğlu, *Mathematica Aeterna* **3(3)**, 221 (2013)